20th Australasian Fluid Mechanics Conference
Perth, Australia
5-8 December 2016

Numerical Investigations of the Wall Shear Stress Behaviour in Curved Coronary Arteries

S. Li[1], C. Chin[1], J. Monty[1], P. Barlis[2] and A. Ooi[1]

[1]Department of Mechanical Engineering
[2]Department of Medicine
The University of Melbourne, Victoria 3010, Australia

Abstract

This paper presents numerical investigations on wall shear stress (WSS) profiles in three-dimensional pulsatile flow through curved stenotic coronary arteries. Clinical evidence has shown that plaque tends to form in the low and oscillatory WSS regions. Direct numerical simulations are carried out in three-dimensional models of the curved arteries with three different degrees of stenosis (0%, 50% and 90%). Low and oscillatory WSS is found near the inner wall of curved artery distal to the stenosis. It is only in the severe stenosis case that a chaotic WSS region is observed downstream of stenosis.

Introduction

Atherosclerosis, also known as atherosclerotic disease, is the most common form of cardiovascular diseases and the direct cause of heart-attack in the community [6]. It is the result of the formation of plaque on the inner artery wall that narrows and hardens a specific region in an artery of the human cardiovascular system. This is clinically known as stenosis. Although the initialisation, development, and progression of atherosclerosis are inevitably associated with system risk factors, such as hypertension, smoking, and hyperlipidemia, the hemodynamic flow fields play an important role as well. One significant implication discovered from recent studies [2, 6] states that regional wall shear stress (WSS) plays a fundamental and important role in the localisation of atherosclerosis and in particular, low and oscillatory WSS ($\pm$0.5 Pa) correlates to the region of localisation of atherosclerosis and the magnitude of low WSS is associated with the severity of atherosclerosis. Likewise, rupture of plaques along with superimposed thrombosis occurs frequently within the coronary atherosclerotic lesion if WSS exceeds the physiologically acceptable WSS range (1-7 Pa [6]) of the normal artery in the clinical definition. Studies by [3] and [9] have found that endothelial cells could be damaged when WSS reaches 40 Pa and stripped if WSS exceeds 100 Pa, resulting in thrombogenesis.

From a clinical perspective, the formation of plaque is more likely to occur in the regions where vessels are curved or irregular. Hence, curved stenotic artery model should be incorporated into the investigations in order for a comprehensive understanding of the blood flow fields and wall shear stress for the diseased coronary artery. Some research have focused on hemodynamics and WSS in the curved coronary artery model. Nosovitsky et al.[7] studied the distributions of velocity and WSS in both steady state and pulsatile flow of a curved artery with several degrees of stenosis using data from computational fluid dynamics. They concluded that higher wall shear stress and velocity are identified at the outer wall for lower stenosis cases while the flow separation was observed at the inner wall downstream of stenosis corresponding with the location of fluctuating WSS for higher degrees of stenosis. Yao et al.[13] investigated hemodynamic changes in arteries with different radii of curvatures and elliptic stenosis using data from numerical simulations. They discussed the influence of curvature and stenosis on the flow resistance and implied the altered WSS behaviour on the wall is because of the presence of secondary flow in the curved model. Liu [4] examined the influence of stenosis located at the inner wall in a curved artery model on pulsatile flow profiles via computational method and found that the flow separation zone correlated with the low and oscillatory WSS downstream of the curved tube when the severity of stenosis reaches certain level, which is likely to promote the restenosis in that area. Liu et al [5] have reconstructed the curved artery models with the progression of stenosis degree from 0 to 90% to study the pulsatile blood flow characteristics by using flow-structure interaction (FSI). They found out that there is a positive correlation between the severity of stenosis and WSS.

Although previous studies have made progress in understanding the flow characteristics in curved stenotic arteries, there has been some limitations in the applicability of the results. In [7], [12] and [10], a turbulence model was introduced to compute flow features, which is less accurate compared with the results from direct numerical simulations (DNS). Only steady-state flow was examined in [13]'s research that was not realistic for actual blood flow. Likewise, the investigations of hemodynamic changes with the progressive amount of stenosis in curved arteries from [5] were not comprehensive given the oscillation of WSS was not examined.

Meanwhile, many studies have examined steady and realistic pulsatile blood flow through stenosed tubes separately. However, the comparison of time-averaged WSS ($\overline{\tau_\omega}$) between the steady-state and pulsatile boundary conditions applied on the same geometry has not been investigated. In light of the computation expense for steady flow, it is of interests to study whether using steady-state inlet boundary to predict the time-averaged WSS behaviour is sufficient.

This study provides a systematic investigation of the change in WSS with the progression of stenosis severity in curved coronary arteries. A realistic physiological pulsatile velocity profile acquired in the proximal artery of a suspected patient with confirmation of unobstructed coronary artery is applied. A comparison of time-averaged WSS between steady and pulsatile conditions is conducted. A fully three-dimensional direct numerical simulation has been conducted to provide a more accurate and comprehensive prediction of flow features in the post-stenotic region.

Methodology

Numerical Model

In this study, the flow is fully three-dimensional, and the fluid is assumed to be Newtonian and incompressible. Thus, DNS of the incompressible Navier-Stokes equations were carried out to investigate WSS behaviour in both steady and pulsatile flow fields of curved artery models for different degrees of stenosis.

The schematic diagram of a curved stenotic artery is displayed in Figure 1. The geometry is adopted from Liu [5]. The length of curvature measured from the outer wall is L_2 = 35.3 mm

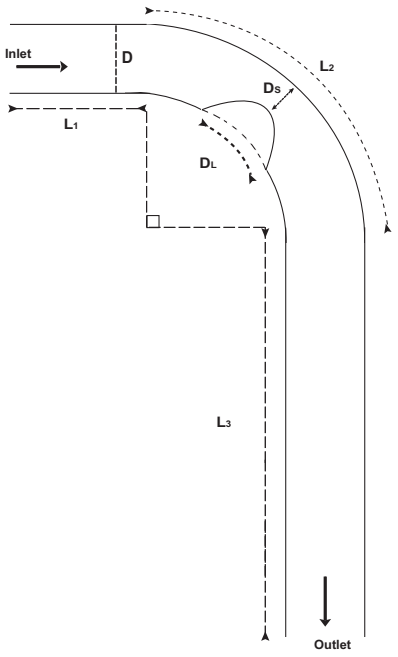

Figure 1: Schematic diagram of curved artery model

S%	0%	50%	90%
D_s (mm)	4.50	3.18	1.42
D_L (mm)	0.00	16.49	27.48

Table 1: The height (D_s) and length (D_L) of the stenosis on the inner wall of a curved coronary artery

with 90 degrees bend. The atherosclerotic plaque formed at the inner wall is located in the middle of the curvature. The height (D_s) and length (D_L) of the plaques for different degrees of stenosis are defined in Table 1. Physiologically, a plaque grows longitudinal and lateral with the decrease of D_s. 10 mm (L_1) and 40 mm (L_3) length straight tube segments are located upstream and downstream of the curvature, respectively. The diameter of artery is D = 4.5 mm and the degree of stenosis (S) is defined as the percentage of blockage of cross-sectional area at the stenosis lesion

$$S = \frac{A_s}{A} \times 100\%. \tag{1}$$

The flow at two different stenosis levels, 50% (moderate) and 90% (severe), were investigated with 0% case as reference. The fluid density is $\rho = 1060$ kg/m^3 and viscosity $\mu = 0.004$ Pa.s, which are similar to the properties of blood. The inlet pulsatile velocity profile is specified in Figure 2 that was obtained from clinical measurement mentioned in [5] to simulate a realistic blood flow motion. In particular, the length of pulsatile period is $T = 1$ s with the mean flow rate to be to be 256.31 ml/min. The Womersley number of the pulsatile profile is calculated according to the following formula:

$$\alpha = r\sqrt{\frac{\omega\rho}{\mu}}, \tag{2}$$

where ω is angular frequency of cardiac cycle. Hence, the corresponding Womersley number fo the cycle was found to be 2.9033. The mean Reynolds number (based on the mean velocity of the cycle $\overline{U}$ and the diameter of the artery D) was 320 with the minimum and maximum between $106 < Re_D < 605$.

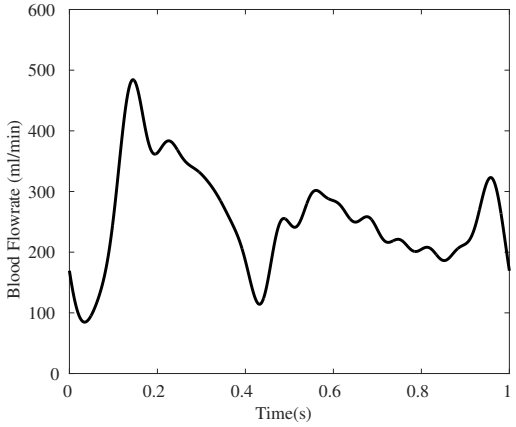

Figure 2: Pulsatile inlet boundary condition profile.

The DNS was conducted using an open source Computational Fluid Dynamics (CFD) code OpenFoam. The size of time step was selected to be Δt = 0.001 s to ensure stability of the simulation. The three-dimensional hexahedral mesh was generated as the computational model. The mesh on the inlet and outlet were created first. A growth layer 17 cells deep with 140 cells in the circumferential direction was applied to the inlet and outlet faces. The thinnest cell (0.02 D) was at the edge and the inner cells had a growth factor of 1.1 in the radial direction. The straight segments grid elements were 0.1 D long in the axial direction and the curved model grid size was 0.1 D long at the widest part of the bend. The curved tube elements were shorter near the inside of the bend in order to preserve the shape of the grid in any given flow-normal cross section. Analysis of mesh resolution accuracy has been conducted and ensured that the current grid mesh is able to help generate precise numerical results. The simulations are carried out over four cycles. The third and forth cycle results are compared and found to be identical. Hence, the forth cycle results are collected for analysis. Validation has been conducted by comparing the numerical data with data obtained in [1]. Very good agreement was found between the numerical and experimental data with less than 2% difference.

Oscillatory Shear Index

Oscillatory shear index (OSI) indicates the temporal oscillation of WSS during the cardiac cycle. It quantifies the change in direction and magnitude of the WSS. The definition for OSI is:

$$\mathrm{OSI} = 0.5 \times \left(1.0 - \frac{\left|\int_0^T \tau_\omega \cdot dt\right|}{\int_0^T |\tau_\omega| \cdot dt}\right), \tag{3}$$

where τ_ω is instantaneous WSS. As indicated in the equation, the range of OSI is from 0 to 0.5, where 0 implies a unidirectional WSS over the cycle while the latter describes a oscillatory flow with a net amount of zero WSS [11]. The importance of OSI in predicting the growth of atherosclerosis has been reported in [11] and [2] that restenosis is likely to occur in the region where high OSI (above 0.15) and low τ_ω ($\pm$0.5 Pa) co-locate. Thus, it is critical to identify where high OSI and low τ_ω occur in the idealised stenotic artery.

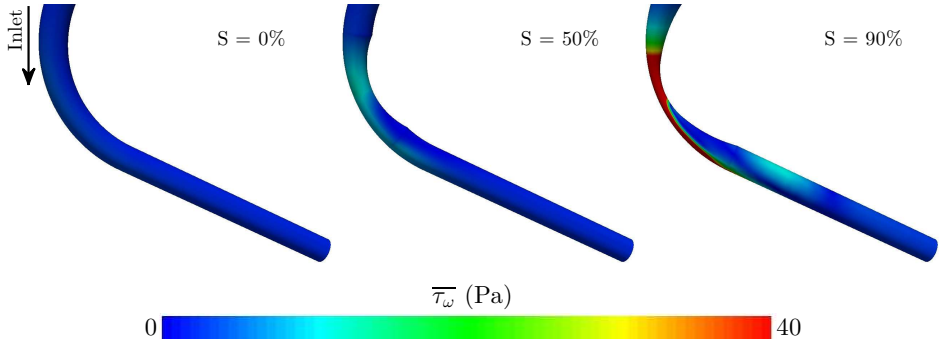

Figure 3: Time-averaged WSS profiles for different degrees of stenosis.

Results and Discussions

Time-averaged WSS ($\overline{\tau_\omega}$)

The $\overline{\tau_\omega}$ profiles for different degrees of stenosis over one pulsatile period are displayed in Figure 3. For all the cases, $\overline{\tau_\omega}$ starts increasing from the inlet of the curved segment. $\overline{\tau_\omega}$ reaches the maximum when the diameter of cross-sectional area reaches D_s. It then sharply drops to the minimum at the inner wall of the stenosis, while on the outer wall $\overline{\tau_\omega}$ gradually decreases throughout the remaining part of the curvature. Downstream of stenosis, $\overline{\tau_\omega}$ profile keeps decreasing on the outer wall until there is a local minimum. It is also notable that with the increasing degree of stenosis, the magnitude of $\overline{\tau_\omega}$ increases accordingly. However, only for S = 90% the $\overline{\tau_\omega}$ exceeds 40 Pa that potentially leads to the rupture of the lesion. Likewise, a chaotic $\overline{\tau_\omega}$ region is identified near the inner wall of the artery downstream of stenosis in S = 90%. The magnitude of $\overline{\tau_\omega}$ is greater than 7 Pa that can lead to thrombosis.

Low and Oscillatory WSS

The time-averaged low WSS fields with the corresponding high OSI are shown in Figure 4. In the 50% case, low $\overline{\tau_\omega}$ occurs immediately after the stenosis indicated in Figure 4 at location A and grows to the post-stenotic region on the inner wall. It is also observed that high OSI area co-locates with a large proportion of low $\overline{\tau_\omega}$ region, where the localisation of plaque formation in the artery can occur. For S = 90%, a few spontaneous regions of low $\overline{\tau_\omega}$ are identified both close to the outlet of the curved segment on the inner wall as well as in the straight part of the artery adjacent to the outlet of curvature. The region of high OSI is discovered on the inner wall of the curvature around the outlet of the stenosis, expanded along the side walls and regenerated on both inner and side walls downstream of stenosis. As a result, the low and high oscillatory $\overline{\tau_\omega}$ areas, where restenosis is likely to be developed, are found both near the end of the stenosis at location B and in the post-stenotic region at location C.

Comparing $\overline{\tau_\omega}$ between steady and pulsatile flows

The spatial-averaged $\overline{\tau_\omega}$ for both steady and pulsatile flows in different stenosis cases are displayed in Figure 5. For steady flow, a parabolic velocity profile was prescribed at the inlet of the model with the same mean flow rate applied in the pulsatile flow.

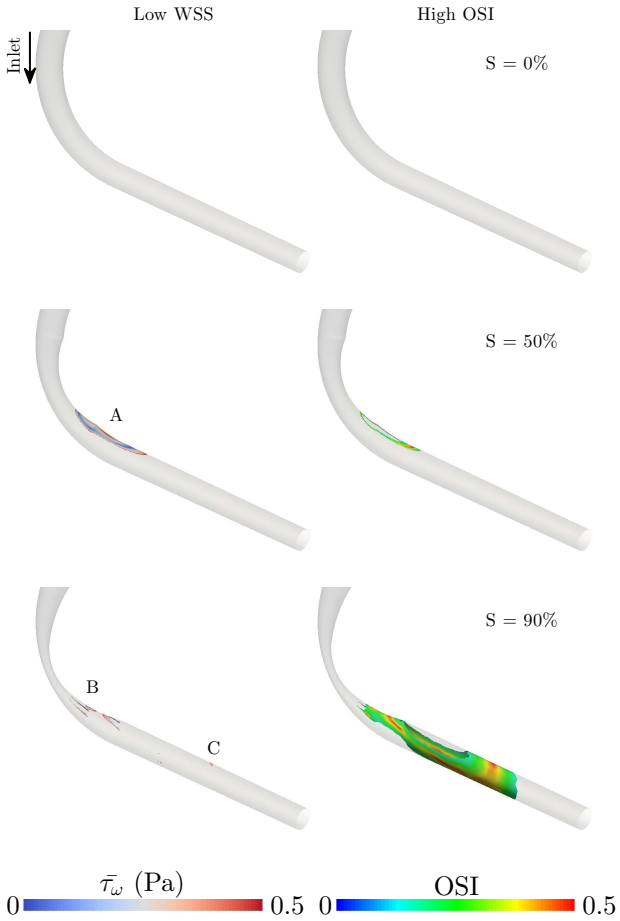

Figure 4: Time-averaged low WSS and corresponding high OSI profiles for different degrees of stenosis.

The results are in agreement for all stenosis degrees with the difference between steady and pulsatile flow less than 0.5%. The percentage of low WSS region over the geometry at the six selected temporal phases at S = 50% varies significantly under the pulsatile condition while remains consistent in steady flow as shown in Figure 6. This implies that certain regions of an artery only experiences low WSS over a portion of one cardiac cycle, where the formation of plaque is likely to occur for long-term's perspective. According to the two sets of the results, it can be stated that although the time-averaged WSS behaviour can be predicted using steady-state flow, more details associated with

the restenosis prediction and diagnosis can only be observed in pulsatile flow.

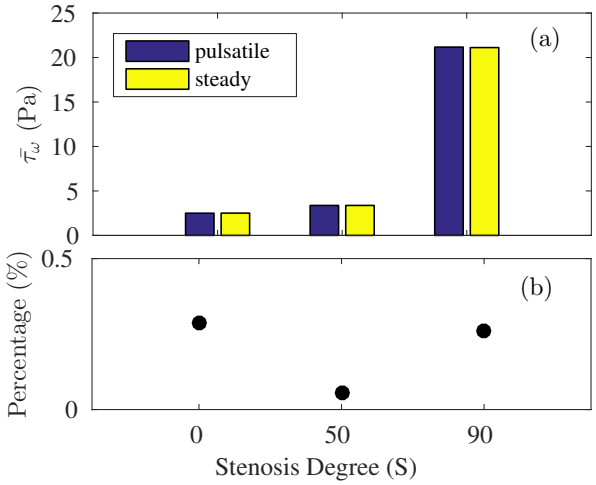

Figure 5: (a) The spatial averaged of $\overline{\tau_\omega}$ for different degrees of stenosis models; (b) The percentage of the difference between steady and pulsatile flows.

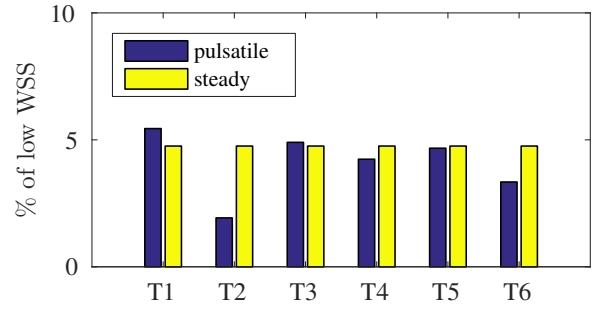

Figure 6: The percentage of the instantaneous low WSS region of steady and pulsatile flows at six time steps of one cardiac cycle for S = 50%

Conclusions

The objective of this study is to understand the WSS behaviour in three-dimensional pulsatile of curved stenotic coronary arteries. Direct numerical simulations are carried out in three different degrees of stenosis. In all the cases, the magnitude of WSS is directly proportional to the degree of stenosis. Likewise, WSS increases steadily from the inlet of curvature and reaches the maximum at D_s, from where it drops to the minimum sharply near the inner wall. Only in severe stenosis case, a time dependent fluctuating WSS region downstream of the stenosis is identified. Low and oscillatory WSS is also found near the outlet of the curved component in the moderate case that indicates the possibility of restenosis region. Meanwhile, the comparison of time-averaged WSS between steady and pulsatile flows indicates that time-averaged WSS can be predicted under steady-state boundary condition while more detailed WSS behaviour in accordance with prediciton and diagnosis can only be predicted using pulsatile flow simulations. Future studies should extend the current work into other degrees of curved stenotic artery models to have a more detailed and systematic understanding of the effect of stenosis degree on the WSS behaviour. Likewise, non-Newtonian blood flow properties should be introduced in the simulations as it is more representative of physiological conditions.

Acknowledgements

The authors would like to acknowledge the support of Australian research Council (ARC) Linkage Project scheme. This research is also supported by the VLSCI under grant number VR0210 on its peak computing facility at the University of Melbourne.

References

[1] Bovendeerd, P.H.M. et al., Steady entry flow in a curved pipe, *Journal of Fluid Mechancis*, **177**, 1987, 233.

[2] Chatzizisis, Y.S. et al., Role of endothelial shear stress in the natural history of coronary atherosclerosis and vascular remodeling: molecular, cellular, and vascular behavior, *Journal of the American College of Cardiology*, **49.25**, 2007, 2379-2393.

[3] Fry, D.L., Acute vascular endothelial changes associated with increased blood velocity gradients, *Circulation Research*, **22.2**, 1968, 165-197.

[4] Liu, B., The influences of stenosis on the downstream flow pattern in curved arteries, *Medical Engineering & physics*, **29**, 2007, 868-876.

[5] Liu, G. et al., Numerical Simulation of flow in Curved Coronary Arteries with Progressive Amounts of Stenosis Using Fluid-Structure Interaction Modelling, *Journal of Medical Imaging and Health Informatics*, **4**, 2014, 605-611.

[6] Malek, A.M., Seth L.A., and Seigo I., Hemodynamic shear stress and its role in atherosclerosis, *JAMA*, **282.21**, 1999, 2035-2042.

[7] Nosovitsky, V.A. et al., Effects of curvature and stenosis-like narrowing on wall shear stress in a coronary artery model with phasic flow, *Computers and Biomedical Research*, **30**, 1997, 61-82.

[8] Ojha, M. et al., Pulsatile flow through constricted tubes: an experimental investigation using photochromic tracer methods, *Journal of fluid mechanics*, **203**, 1989, 173-197.

[9] Ramstack, J.M., Zuckerman, L., and Mockros, L.F., Shear induced activation of platelets, *Journal of Biomechanics*, **12.2**, 1979, 113-125.

[10] Ryval, J., Straatman A.G., and Steinman, D.A., Two-equation turbulence modeling of pulsatile flow in a stenosed tube, *Journal of biomechanical engineering*, **126.5**, 2004, 625-635.

[11] Soulis, J.V. et al., Oscillating shear index, wall shear stress and low density lipoprotein accumulation in human RCAs, 2011.

[12] Varghese, S.S. and Steven, H.F., Numerical modeling of pulsatile turbulent flow in stenotic vessels, *Journal of biomechanical engineering*, **125.4**, 2003, 445-460.

[13] Yao, H. et al., Computational modelling of blood flow through curved stenosed arteries, *Journal of Medical Engineering & Technology*, **24.4**, 2000, 163-168.